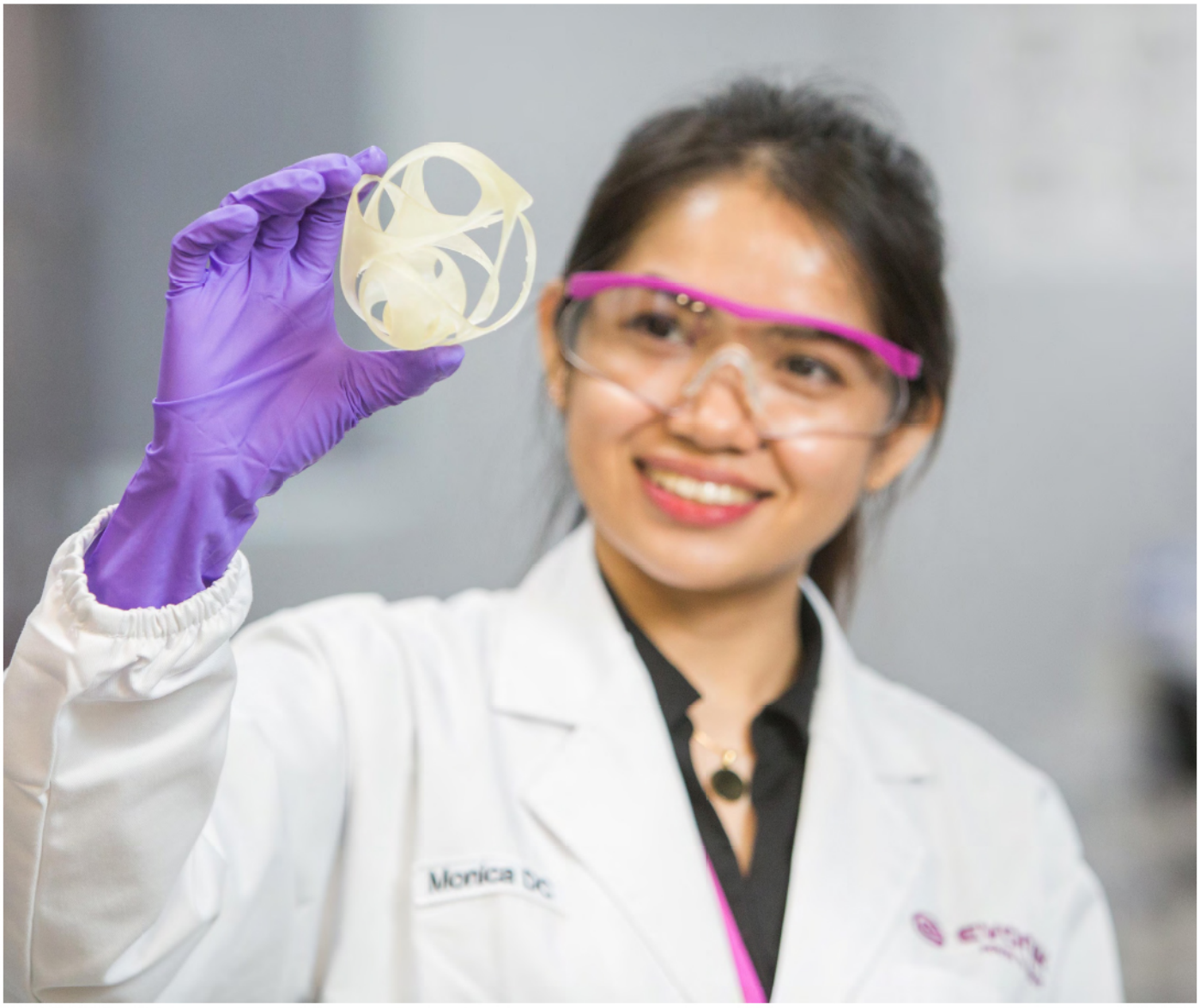

Pushing the boundaries of chemistry? It takes #HumanChemistry

Make your curiosity and talent as a chemist matter to the world with a specialty chemicals leader. Together, we combine cutting-edge science with engineering expertise to create solutions that answer real-world problems. Find out how our approach to technology creates more opportunities for growth, and see what chemistry can do for you at:

evonik.com/career

EVONIK
Leading Beyond Chemistry

Received: 8 July 2020 | Revised: 30 September 2020 | Accepted: 2 October 2020

DOI: 10.1002/app.50136

ARTICLE

Applied Polymer Science WILEY

Body-temperature shape-shifting liquid crystal elastomers

Rajib K. Shaha[1] | Amir H. Torbati[2] | Carl P. Frick[1]

[1]Department of Mechanical Engineering, University of Wyoming, Laramie, WY, USA

[2]Department of Mechanical Engineering, University of Colorado Denver, Aurora, CO, USA

Correspondence
Rajib K. Shaha, Department of Mechanical Engineering, University of Wyoming, Laramie, WY 82071, USA.
Email: rshaha@uwyo.edu

Funding information
National Science Foundation, Grant/Award Number: NSF-PFI 1827288

Abstract

Nematic monodomain liquid crystal elastomers (LCEs) undergo efficient temperature-induced reversible shape-shifting around the nematic-isotropic transition temperature (T_{ni}) due to the presence of the liquid-crystalline order of mesogens. Usually, the T_{ni} of nematic LCEs is much higher than the human body temperature, and therefore LCEs are not often considered for biomedical applications. This study describes an LCE system where the T_{ni} is tuned by substitution of the rigid mesogens RM257 with a flexible backbone PEGDA250. By systematically substituting the RM257 with PEGDA250, the T_{ni} of LCEs was observed to decrease from 66°C to 23°C. A rate-optimized LCE material was fabricated with 10 mol % rigid mesogens substituted with a flexible backbone that demonstrated T_{ni} at 32°C, in-between the room temperature of 20°C and the body temperature of 37°C. The T_{ni} allowed the programmed shape at room temperature, quick shape-shifting upon exposure to body temperature, and before-programmed shape when kept at body temperature. This LCE material displayed reversible length change of 23%, opacity change, and shape change between room temperature and body temperature.

KEYWORDS

biomaterials, elastomers, liquid crystals, structure-property relationships, thermal properties

1 | INTRODUCTION

Liquid crystal elastomers (LCEs) have emerged to be an efficient shape-reversible polymer due to a facile phase transformation stemming from their inherent liquid crystalline order and the crystalline structures.[1,2] LCEs combine liquid crystal orientational order and elastomer entropic elasticity to give rise to interesting behaviors such as soft elasticity, anisotropy, and large reversible actuation.[3] Since the conception of the liquid crystal elastomers, various novel engineering applications have been proposed based on the reversible actuation including actuators,[4–6] soft robotics,[7,8] optical elements[9] and mechanical damping.[10,11] Additionally, LCEs are proposed for biomedical applications such as artificial muscle,[12–14] scaffolds for tissue engineering,[15] drug-delivery vehicles,[16] vascular implants,[17] interbody fusion cages[18] and synthetic intervertebral disc.[19] However, the proposed biomedical applications mostly focused on either the non-actuation behavior or externally controlled shape-activation.

In LCEs, the 'liquid crystallinity' stems from the presence of rigid molecules called mesogens in a loosely cross-linked elastomeric network. LCE molecular organization can generally be categorized in either the nematic phase where the mesogens have relatively one-dimensional orientational order, or in the isotropic phase where the mesogens are randomly oriented. For LCEs in the nematic state, the mesogen order can further be classified into two configurations – (1) polydomain where the mesogens form localized ordered domains on the order of microns in size,[20–22] and (2) monodomain where the mesogens are ordered along a self-similar direction across the entire LCE specimen. The shape-recovery actuation

demonstrated by LCEs are a result of the reversible phase transformation between the nematic-monodomain and isotropic phases, that is, the mesogens transition from long-range order to random orientation, which is entirely reversible (Figure S1). This nematic-isotropic transition also affects the opacity of the sample, since the ordered and disordered mesogens block or allow the transmission of light through LCEs, respectively. The nematic-isotropic transition of LCEs can be achieved using external stimuli such as light,[9] magnetic field,[23] solvent,[24] and heat.[3] Nevertheless, heat stimulation to induce shape-shifting can be a reliable and straightforward approach to achieve actuation functionality.

Historically, LCEs have seen limited use in potential applications, in large part due to synthesis issues. Various complex fabrication schemes have been employed to achieve monodomain LCEs[25], however, these schemes are usually limited to small sample thickness due to lack of robust mesogen alignment method; or the scheme suffers from low repeatability due to poorly defined intermediate steps.[1,26] A method recently introduced by Yakacki et al. demonstrated the capability of fabrication of bulk LCE specimens with highly repeatable properties.[3] This method utilizes two-stage orthogonal reaction schemes to fabricate shape-shifting LCEs. During first-stage, a thiol-acrylate Michael addition reaction creates nematic polydomain LCEs. During the second-stage, the locally ordered mesogens in polydomain LCEs are aligned by mechanically stretching, and a radical photopolymerization reaction fixes the stretched shape to achieve monodomain LCEs. This two-stage fabrication method allows for relatively straightforward manufacture of LCEs on the millimeter scale and above, and was adopted to prepare LCEs in this study.

Unfortunately, for potential biomedically-related applications, the nematic-isotropic transition temperature is typically upwards from 70°C.[27,28] Recently, only a few researchers have reported LCEs that undergo nematic-isotropic transition at a lower temperature.[16,28] Inoue et al. fabricated a novel LCE system that shifts diffusivity, rather than shape, at body temperature.[16] Saed et al. developed a system of LCEs with highly tailorable nematic-isotropic transition temperature that utilized different mesogens, oligomerization prior to cross-linking and different cross-linking reactions[28]; however, their method is relatively cumbersome, required intermediate steps, and they did not explore the shape-actuation at body temperature. Therefore, there is no existing LCE system for the body-temperature shape-shifting application that can be fabricated using commercially available monomers, and this study aims to develop one.

The most critical aspect of developing a body-temperature LCE material is the tailoring of the nematic-isotropic transition temperature to be around body temperature. The nematic-isotropic transition of LCEs are usually affected by many factors such as the cross-linking of the network,[27,29–31] network homogeneity,[28,32] type of mesogens, that is, main-chain or side-chain,[33,34] the size of the mesogens,[28,35] the structure of mesogens,[31] the type and size of network spacer,[18,36] mesogen concentration,[28] applied stress for mesogen alignment,[37,38] the network formation temperature[39] and the presence of solvent during network formation.[40] However, the size of the mesogens was found to be one of the most critical factors to affect the transition temperature.[28,35] Therefore, in this study, we pursued substitution of rigid mesogens with a flexible backbone (hence decreasing the mesogen concentration and increasing the spacing between the mesogens), in order to lower the nematic-isotropic transition temperature. Polyethylene glycol diacrylate was chosen as the flexible backbone as it is widely used in biocompatible systems.[41] Ultimately, an LCE with potential for biomedical applications was obtained that undergoes a nematic-isotropic transition in-between room temperature and body temperature. The rationale for this was that the highest actuation rate of LCEs, with respect to temperature, happens near the nematic-isotropic transition temperature,[27] such that the shape-shifting can occur in seconds instead of minutes. Therefore, for efficient shape-shifting application, the nematic-isotropic transition temperature needs to be in the vicinity of the application temperature. For biomedical applications, this transition temperature is required to be around human body temperature, that is, 37°C. For a robust application, this temperature is most preferably be in between the room temperature and the body temperature such that the shape can be programmed and stored in the nematic phase at room temperature and subsequently applied at body temperature where the isotropic phase will be stabilized. Aiming towards developing a body temperature shape-shifting LCEs, this work followed the following steps- (1) systematically substitute rigid mesogens with flexible backbone, (2) study the effect of rigid mesogen substitution with a flexible backbone on nematic-isotropic transition temperature, and (3) identify an LCE system that demonstrates actuation and opacity transition near body temperature.

2 | MATERIALS AND METHODS

2.1 | Materials

A two-stage Michael Addition and Photopolymerization scheme was applied to fabricate the LCE (Figure 1), as described in previous studies.[3,27] The constituent

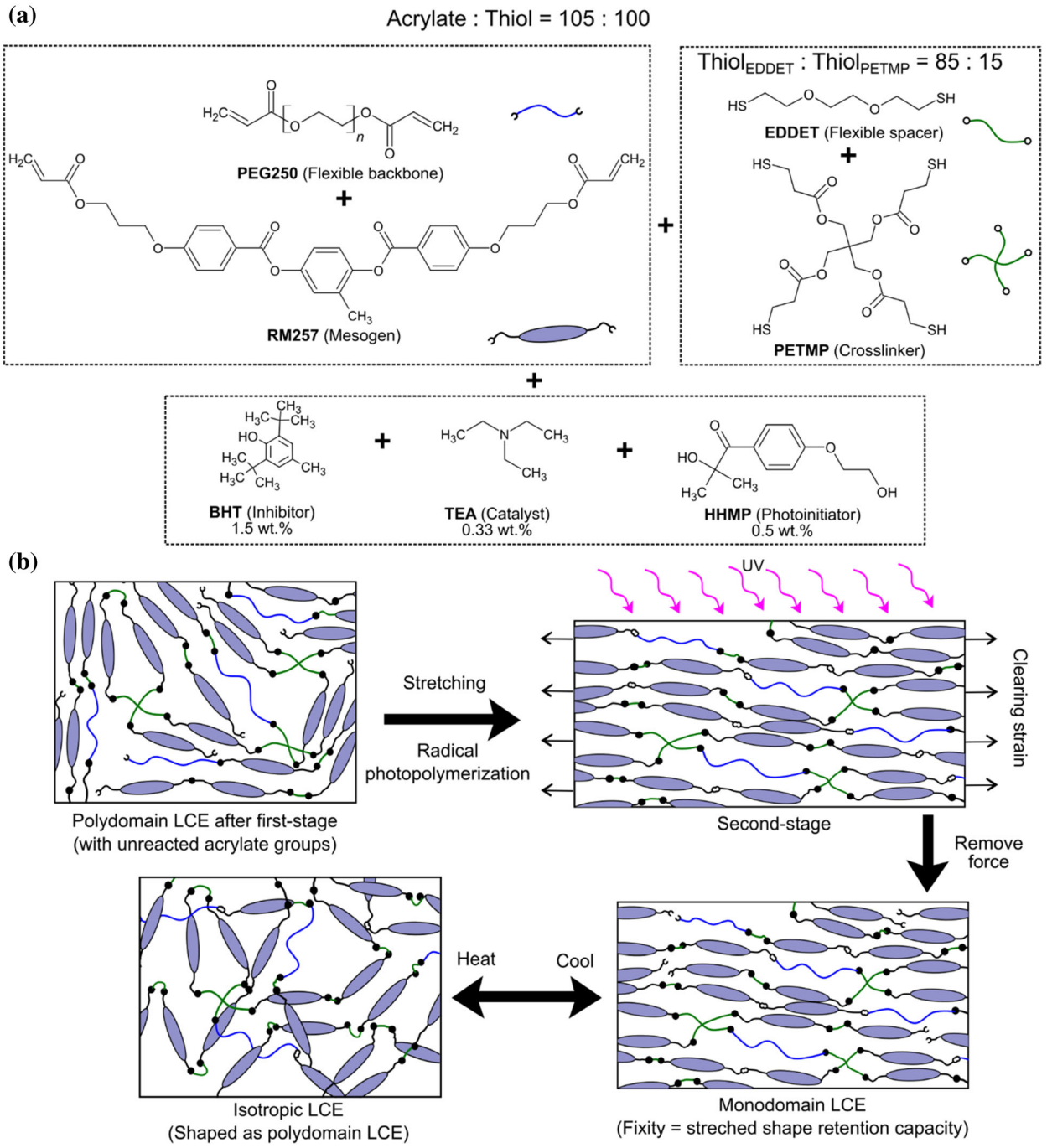

FIGURE 1 (a) Schematic of the chemicals used in the fabrication of LCE. A two-stage fabrication scheme was employed - first Michael Addition reaction, followed by a radical Photopolymerization reaction. The acrylated rigid mesogens (RM257) were systematically substituted with acrylated flexible backbone (PEG250). Thiol-functionalized flexible spacer (EDDET) and cross-linker (PETMP) was used to form the network. Catalyst (TEA) and inhibitor (BHT) were used to initiate and control the reaction rate, respectively. Photoinitiator (HHMP) was used to carry out second-stage photopolymerization. The ratio of acrylate to thiol functional groups was 105:100, that is, 5% excess acrylate than the stoichiometric amount was used. PETMP contributed to 15% of all thiols, which refers to the degree of cross-linking. (b) Schematic diagrams show the polydomain LCE with unreacted acrylate groups after the first-stage Michael Addition reaction. Mesogens are aligned by mechanical stretching and UV photopolymerized to create monodomain LCE fixed at the stretched shape. Fixity indicates retention capacity of stretched shape when the applied force is removed. A reversible phase transition occurs between monodomain-nematic and isotropic LCE by heating and cooling. The schematics in this figure are adapted from Shaha et al., 2020[19]. LCE, liquid crystal elastomers [Color figure can be viewed at wileyonlinelibrary.com]

chemicals were obtained commercially and used without additional processing. The mesogenic network backbone 1,4-Bis-[4-(3-acryloyloxypropyloxy) benzoyloxy]-2-methylbenzene (RM257) was procured from Wilshire Technologies, Inc. (Princeton, NJ, USA). The flexible network backbone Poly(ethylene glycol) diacrylate (PEG250, Mn 250), bifunctional flexible spacer 2,2-(ethylenedioxy) diethanethiol (EDDET) and tetra-functional cross-linker pentaerythritol tetrakis (3-mercaptopropionate) (PETMP) were obtained from Sigma-Aldrich, Inc. (St. Louis, MO, USA). The base catalyst triethylamine (TEA), inhibitor 2,6-di-tert-butyl-4-methylphenol (BHT) and photoinitiator 2-hydroxy-4′-(2-hydroxyethoxy)-2-methylpropiophenone (HHMP) were also purchased from Sigma-Aldrich.

2.2 | LCE fabrication

The first-stage of the LCE fabrication led to network formation using a base-catalyzed Michael Addition reaction scheme. The second-stage involved programming shape-memory of the LCE samples utilizing radical photopolymerization. At first, the RM257 and BHT were melted at 120°C using a convection oven. The PEGDA, EDDET, PETMP, HHMP, and TEA was added to the melt and mixed in steps by further heating and mixing using a vortex mixer (Vortex Genie 2, VWR, Radnor, PA, USA). The molar ratio of the acrylate functional group contributing chemicals, that is, RM257 and PEGDA, was varied to achieve network with various mesogen concentrations (Figure 1(a)). The samples were named as "RM" followed by RM257 mole proportion – "PEG" followed by PEGDA mole proportion (Table 1). For example, RM90-PEG10 indicates 90% of acrylate groups are contributed by RM257. LCEs with five different compositions – RM100-PEG0, RM95-PEG5, RM90-PEG10, RM80-PEG20, and RM0-PEG100 were fabricated. The ratio of the chemicals containing thiol functional groups, that is, EDDET and PETMP, was kept constant such that 15% of the total thiol functional group was contributed by the cross-linker PETMP. Furthermore, the ratio of the acrylate and thiol functional groups containing chemicals were chosen such that the acrylate groups are present at 5% in excess than the stoichiometric amount. The amount of BHT (1.5 wt%), HHPM (0.5 wt%), and TEA (0.33 wt%) were calculated based on the total weight of the acrylate and thiol monomers. The LCE forming mixture was degassed under 22 in-Hg vacuum until no visible air bubbles were present and transferred to molds made of glass slides with 1 mm thick polytetrafluoroethylene spacers. The mold was kept at 100°C for 12 hours to allow the first-stage Michael Addition reaction to complete. The transparent LCE samples were extracted from the mold and cooled to room temperature to enable mesogens to self-assemble to nematic polydomain conformation. The RM100-PEG0, RM95-PEG5, and RM90-PEG10 turned opaque white, while the RM80-PEG10 and RM0-PEG100 samples remained transparent at room temperature.

The polydomain LCE samples with unreacted acrylate function groups, obtained after the first-stage, were mechanically stretched to align the mesogens to the loading direction (Figure 1(b)). The stretching caused the samples to become transparent and temporarily monodomain. This stretching required to transform from opaque white to transparent is often referred to as clearing strain. In addition to the visual observation, the appropriate amount of stretching to be applied for maximum mesogen alignment, defined as applied strain ($\varepsilon_{applied}$) in this study, was determined by uniaxial tensile testing. The polydomain LCE samples with $5 \times 1 \times 20$ mm^3 dimensions, obtained after the first-stage, was tested under tension at room temperature using a dynamic mechanical analyzer (DMA Q800, TA Instruments, New Castle, DE, USA). At least four samples were tested for each material. For RM100-PEG0, RM95-PEG5 and RM90-PEG10, the $\varepsilon_{applied}$ was identified from the stress–strain curve as the inflection point between the plateau region at the middle and the linear region at the end (Figure 2(a)). The RM80-PEG20 did not show an obvious stress–strain plateau and an arbitrarily high $\varepsilon_{applied}$ was chosen. The mesogen alignment in the monodomain LCE, hence the shape of the sample, was made permanent by radical photopolymerization of the unreacted acrylate functional groups in the stretched

TABLE 1 LCE with various mesogen and flexible backbone compositions and their corresponding average transition temperatures

Sample	$Acrylate_{RM257}$: $Acrylate_{PEG250}$	T_g(°C)	T_{ni}(°C)
RM100-PEG0	100: 0	4	66
RM95-PEG5	95: 5	3	52
RM90-PEG10	90: 10	3	32
RM80-PEG20	80: 20	−2	23
RM0-PEG100	0: 100	−40	–

Abbreviation: LCE, liquid crystal elastomers.

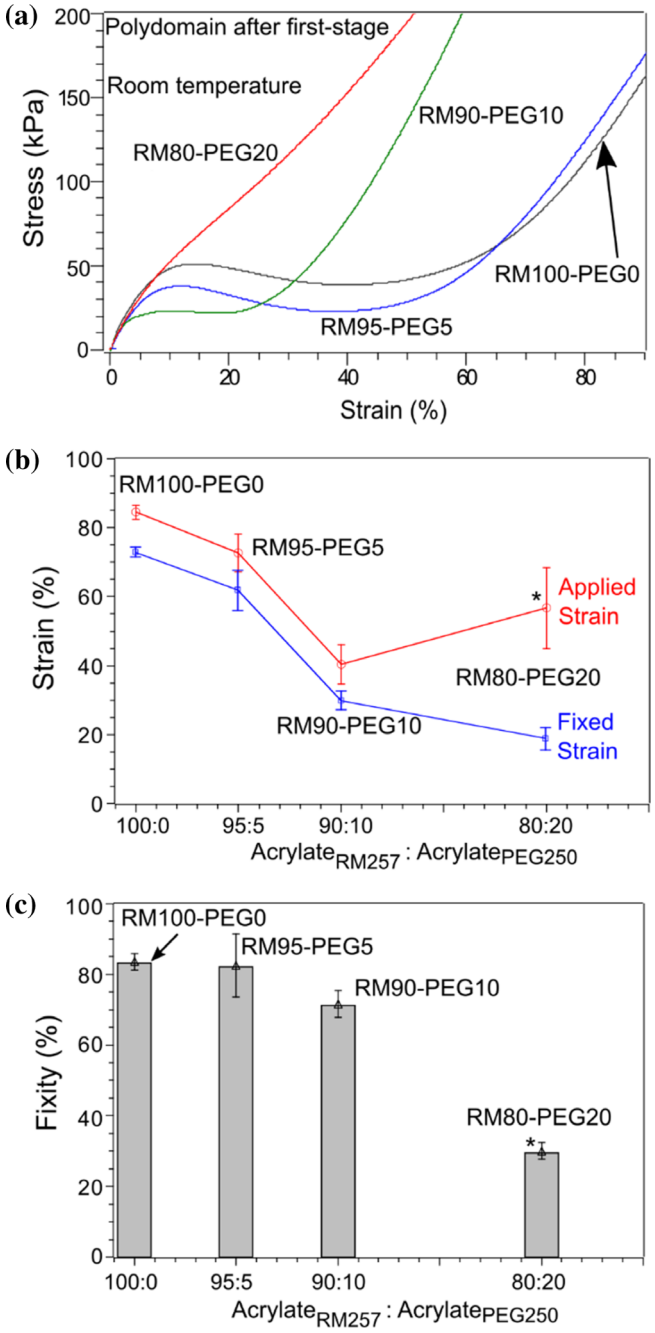

FIGURE 2 (a) Representative monotonic tensile behavior of polydomain LCE with unreacted acrylate groups after first-stage Michael addition reaction. Samples were tested at room temperature. Samples showed decreasing soft elasticity with decreasing RM257–PEG250 ratio. The applied strain was determined as the beginning of the linear rubbery elastic region at the higher strain end. (b) Average applied strain and fixed strain are shown as a function of the ratio of rigid mesogens to the flexible backbone. In general, both applied strain and fixed strains decreased with increasing flexible backbone PEG250. Only for RM80-PEG20, an arbitrarily high applied strain was chosen, indicated by an asterisk (*). (c) Average fixity is shown as a function of the ratio of rigid mesogen to the flexible backbone. The asterisk (*) indicates that the fixity was calculated based on the arbitrarily chosen applied strain for RM80-PEG20. In all cases, the error bars represent the standard deviation from at least four tests. LCE, liquid crystal elastomers [Color figure can be viewed at wileyonlinelibrary.com]

shape (second-stage) (Figure 1(b)). As no mesogen was present, the RM0-PEG100 sample was photopolymerized without any stretching after first-stage. The radical photopolymerization was carried out by exposing the samples to 365 nm wavelength ultraviolet light (Blackray B-100A/R, UVP, Upland, CA, USA) for approximately 1 hour to photopolymerize the excess acrylate functional groups. The duration of the first-stage Michael Addition reaction and the second-stage radical photopolymerization is considered long enough to achieve the maximum conversion from the procedures described in the previous studies.[3,27] After the second-stage reaction, monodomain LCE samples with $5 \times 0.85 \times 20$ mm^3 dimensions were obtained.

In addition to the monodomain film samples, twisted polydomain and fixed polydomain samples were fabricated from the RM90-PEG10, for shape change and opacity change demonstrations. Instead of stretching after first-stage, the samples were twisted and UV photopolymerized to obtain twisted polydomain samples. The fixed polydomain samples were UV photopolymerized without any deformation after first-stage.

2.3 | Fixity

The degree of programmed shape-retaining capacity, that is, fixity, was measured for all LCE materials. The polydomain samples with unreacted acrylate groups after first-stage were thermally cycled through the T_{ni} and cooled to room temperature to reset any deformation during removal from the mold. The initial lengths of the samples were recorded. The samples were stretched to the applied strains ($\varepsilon_{applied}$) and photopolymerized to make the monodomain shape permanent. The monodomain samples were again thermally cycled through the T_{ni} to room temperature, and their final length was measured. The fixed strain (ε_{fixed}) was calculated from the final and the initial lengths. The fixity was defined as the ratio of ε_{fixed} and $\varepsilon_{applied}$ (Equation 1). All the measurements were taken for at least four samples of each material.

$$Fixity = \frac{\varepsilon_{fixed}}{\varepsilon_{applied}}. \quad (1)$$

2.4 | Polarized optical microscopy

The polarized optical microscopy (POM) images of monodomain LCEs were taken using an Olympus BX-51 microscope equipped with a cross-polarizer-analyzer (Olympus, Center Valley, PA, USA). The samples were

placed between the polarizer and analyzer and imaged with the light transmitted through the samples. The presence of birefringence was used to determine the existence of the liquid crystalline order in the material.

2.5 | Dynamic mechanical properties and phase-transitions analysis

Dynamic properties and the phase transitions of LCE film samples were studied under dynamic tensile load using DMA Q800. The LCE samples of approximately $5 \times 0.8 \times 20\ mm^3$ dimensions were thermally cycled through the T_{ni} before testing to reset any deformation history. Each material was tested at least in duplicates. The samples were mounted in tensile grips and cooled to −20°C, well below the glass transition temperature. The samples were kept isothermal for 10 mins to allow thermal equilibrium and ramped at 0.5°C/min to 120°C, well beyond the T_{ni}. The other test parameters were chosen as 0.01 N preload force, 0.1% oscillating strain at 1 Hz frequency, and 125% force track. The slow temperature ramp rate allowed uniform temperature throughout the sample during the test. The force track value was applied to compensate for the change in sample length while the experiment is running. The amplitude of oscillating strain was chosen from a preliminary strain sweep test (data not shown here) such that the sample deformation is limited in the linear viscoelastic region. The dynamic properties such as storage modulus (E') and loss tangent (tan δ), and the temperature (T) was measured and recorded by the DMA. The storage modulus and loss tangent were plotted against the temperature to determine the transition temperatures for the LCE films. The glass transition temperature (T_g) and the nematic-isotropic transition temperatures (T_{ni}) were determined from the storage modulus as a function of temperature and tan δ as a function of temperature plots. The T_g was defined as the temperature where the tan δ value was maximum, and the T_{ni} was defined where the E' value was minimum, measured using Universal Analysis software (UA 2000, TA Instrument, New Castle, DE, USA).

2.6 | Actuation

The shape actuation of the LCE samples was assessed using the DMA. Each material was tested at least in duplicates. The tensile grips were used to clamp the samples with their mesogen alignment (i.e., stretching direction) along the loading axis. The samples were heated beyond their respective T_{ni} and allowed to equilibrate at the isotropic phase for 10 min. The samples were cooled at 0.5°C/min to −25°C and the change in length was recorded, while a 0 N axial load was maintained. The actuation strain was calculated with respect to the sample length at the isotropic phase and plotted against temperature. The length change, that is, actuation strain and the rate of length change was also calculated between 20°C and 30°C using Universal Analysis software.

2.7 | Shape-shifting test

The thermal actuation, shape-shifting, and opacity-shifting of the LCE samples were studied using RM90-PEG10 monodomain, twisted polydomain, and fixed polydomain samples, respectively. The samples were thermally cycled around 32°C (i.e., T_{ni}) of RM90-PEG10, by placing in approximately 20°C and 37°C water bath. The transitions of the samples were photographed and video recorded while submerged in both water baths.

3 | RESULTS

3.1 | LCE fabrication

The LCEs for this study were fabricated following a two-stage Michael addition and photopolymerization method (Figure 1). In the first-stage, the acrylate functional group-containing monomers (i.e., mesogens and flexible backbone) were reacted with the thiol functional group-containing monomers (i.e., flexible spacer and cross-linker) (Figure 1(a)). The first-stage resulted in a polydomain LCE network with unreacted acrylate functional groups. The samples were mechanically stretched to align mesogens, and the unreacted acrylate functional groups were bonded with each other in the second-stage via photopolymerization (Figure 1(b)). The final result is a monodomain LCE. The molar ratio of the mesogens and the flexible spacer was varied, with the thiol fraction being constant, to investigate the effect on the nematic-isotropic transition temperature and the shape-shifting of the LCE. The LCE samples with varying relative molar ratio of the rigid mesogen to the flexible backbone are listed in Table 1. For example, the RM90-PEG10 sample contained 90 moles % of rigid mesogen RM257, and the rest 10 moles % was substituted with flexible backbone PEGDA250. In addition to monodomain samples, twisted (i.e., partially deformed) polydomain and fixed (i.e., undeformed) polydomain LCE samples were fabricated to probe the shape-shifting and opacity-shifting around body temperature.

When the monodomain LCEs are heated, a phase transformation is induced, and the mesogens start to lose alignment from the global orientation. The order disintegration increases dramatically as the temperature nears the nematic-isotropic transition and becomes random above the nematic-isotropic transition temperature.[21,29,42] During the length actuation process, the elongated monodomain material transitions to the pre-elongation shape, hence, showing contraction along stretching direction, and expansion along the perpendicular to the stretching direction. Besides actuation, LCEs also demonstrate the change in opacity, when the transition occurs between nematic-polydomain and isotropic phases. The many locally ordered domains of the polydomain LCEs scatter and effectively block light, hence are opaque.[43] However, when the LCEs become isotropic, all the mesogens become transparent as the randomly oriented individual mesogens do not scatter light considerably and appear transparent.[43]

3.2 | Fixity

The strain requirement for maximum alignment of mesogen domains, termed as applied strain, were studied from the monotonic tensile test of polydomain LCE with unreacted excess acrylate. The representative stress–strain plots for different materials are shown in Figure 2 (a). The stress–strain plot for RM100-PEG0 (i.e., LCE with no mesogen substitution) showed similar behavior as observed previously for LCEs.[27,30,40] At strains less than approximately 10%, the stress–strain plot showed the initial viscoelastic behavior. In between approximately 10%–75% strain, the curve showed a plateau. This plateau is frequently observed for LCEs, termed the soft elastic region where the mesogen domain rotation was the dominating deformation mechanism. The soft elastic region was followed by the rubbery elastic region, similar to the conventional elastomer, where network chains are stretched. With the increase in the amount of the flexible PEG backbone, the span of the soft elastic plateau became dramatically shorter, to almost zero for RM80-PEG20. The shorter soft elastic plateau indicates the presence of domains with less ordered mesogens, hence, a smaller strain is enough for achieving mesogen alignment.

The applied strain was determined as the inflection point between the soft elasticity plateau and the rubbery-elastic section at the end of the stress–strain curve, to ensure maximum mesogen alignment. The samples were also observed to become transparent at this strain, in contrast with the opaque white unstretched polydomain LCEs. The RM0-PEG100 showed relatively brittle behavior and failed on average at 10% strain, not shown in Figure 2(a). The RM100-PEG0, RM95-PEG5, RM90-PEG10, and RM80-PEG20 samples could sustain much higher strain and did not fail up to 90% strain.

The average applied strain was plotted as a function of the ratio of rigid mesogen RM257 to the flexible backbone PEG250 (Figure 2(b)). The applied strain substantially diminished by lowering the rigid RM257 content, from around 85% strain for RM100-PEG0 to nearly 40% strain for RM90-PEG10. Because RM80-PEG20 did not show any obvious soft elastic plateau during the tensile test (Figure 2(a)), a strain of approximately 55% was used as applied strain, which is more than sufficient to ensure maximum mesogen alignment. After the second-stage reaction, the nematic monodomain LCEs partially relax the programmed shape, described by the fixed strain. The fixed strain was also plotted with respect to the ratio of rigid mesogen RM257 to the flexible backbone PEG250 (Figure 2(b)). The fixed strain decreased considerably from around 74% strain for RM100-PEG0 to nearly 19% strain for RM80-PEG20.

Consistent with previous studies investigating LCEs, the fixity was calculated as the ratio of the fixed strain and the applied strain.[27,40] The average fixity plotted as a function of the ratio of RM257 to PEG250 is shown in Figure 2(c). The fixity slightly decreased from 87% for RM100-PEG0 to 75% for RM90-PEG10. Noting that arbitrarily high applied strain was chosen for RM80-PEG20, the fixity measurement of 34% may not directly be comparable to other materials. The fixity was not measured for LCEs with RM257 content less than 80% as the shape could not be programmed due to their brittle nature and lack of soft elasticity.

3.3 | Polarized optical microscopy

The polarized optical microscopy (POM) was conducted on the monodomain LCE samples after the second-stage to study the presence of the liquid crystalline order. The representative POM images of LCEs with varied rigid mesogen to flexible backbone ratios are shown in Figure 3. The bright images under cross-polarizer for RM100-PEG0, RM95-PEG5, RM90-PEG10, and RM80-PEG20 indicated the birefringence properties of these monodomain LCEs. However, the RM0-PEG100 sample was dark under cross-polarized light. The birefringence is an indication of the presence of liquid crystalline order.[9,36,40,44,45] The RM0-PEG100 samples consisted of only flexible backbones and, did not show any birefringence. All other samples had mesogens present in their backbone and consequently showed birefringence.

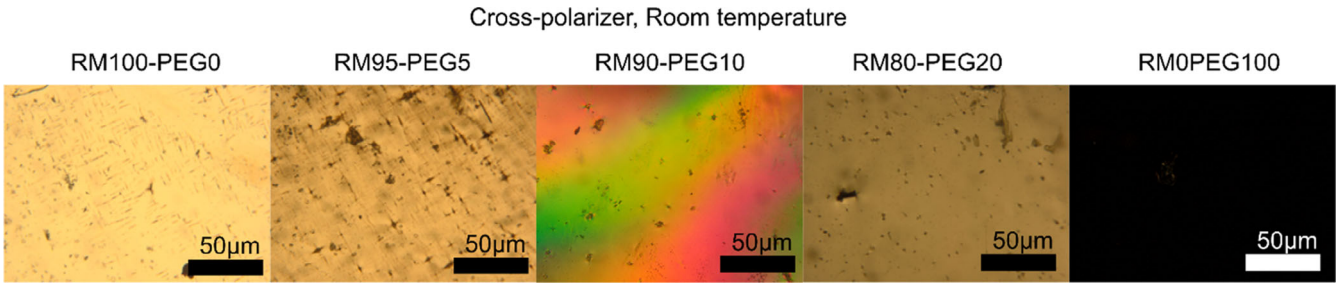

FIGURE 3 Polarized optical microscope images of representative monodomain LCE films taken at room temperature. All the samples, other than RM0-PEG100 (i.e., no liquid crystals, rather 100% flexible backbone), demonstrate birefringence under cross-polarizer. The birefringence indicates the presence of liquid crystalline order. LCE, liquid crystal elastomers [Color figure can be viewed at wileyonlinelibrary.com]

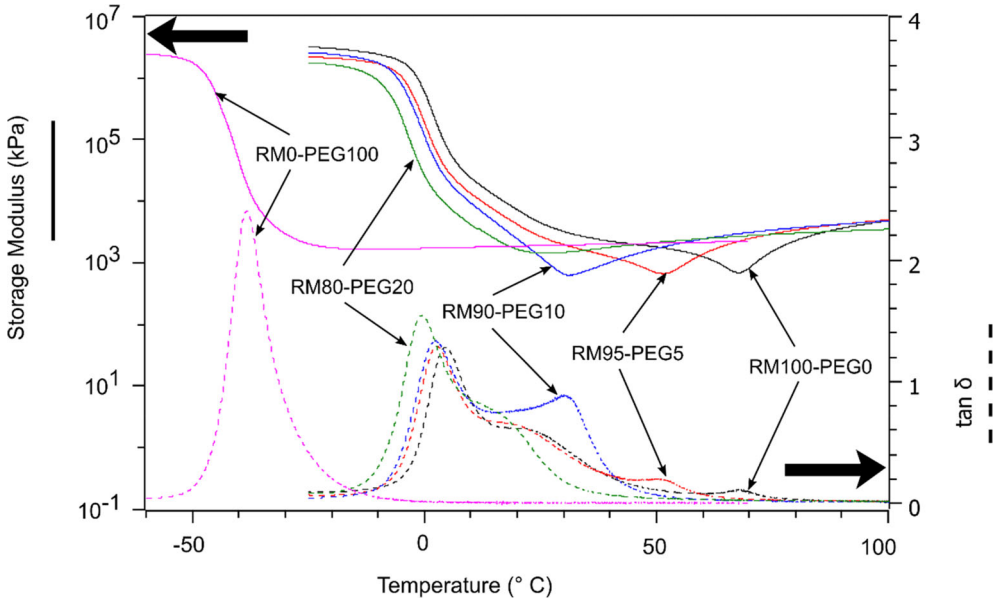

FIGURE 4 Representative storage modulus and tan δ plots as functions of temperature, obtained from the dynamic mechanical analysis of monodomain LCE with varied rigid mesogen to flexible backbone ratio. The isotropic transition temperature decreased with increased mesogen substitution. RM90-PEG10 (i.e., LCE with 10% mesogen substituted) demonstrated the isotropic transition at an approximate temperature slightly below the human body temperature of 37°C. LCE, liquid crystal elastomers [Color figure can be viewed at wileyonlinelibrary.com]

3.4 | Dynamic mechanical analysis

Dynamic mechanical analysis (DMA) was conducted for all samples to study the LCE behavior as a function of temperature, including the phase transition temperatures. Representative storage modulus (E') as a function of temperature (T) and tan δ as a function of temperature (T) plots for all the compositions investigated are available in Figure 4. The RM100-PEG0 (i.e., LCE with no mesogen substitution) sample showed similar behavior as observed previously for LCEs.[27,30,40] At temperatures below approximately 0°C, the storage modulus and the corresponding tan δ plot exhibited plateau regions, indicating glassy behavior typical to polymers. In the glassy region, exceptionally high E' in the order of 10^6 kPa and low tan δ value of around 0.1 occurred due to limited motion of LCE network chains, and consequent high elastic deformation of LCE.[10,27] With the increase in temperature, the network undergoes a classic glassy-to-rubber transition associated with a sharp drop in E' by several orders of magnitude and an increase in tan δ. With further increase in temperature, the tan δ increased to peak values above 1.2, indicating the ratio of energy dissipation and energy storage capacities by the network reached the maximum. The tan δ dropped again with increasing temperature as the energy dissipation capacity of the network diminished due to increasingly free movement between chains, and the network became rubbery-nematic. The peak of the tan δ vs. temperature plot is defined as the glass transition temperature, T_g.

Above T_g, the decreasing E' of rubbery-nematic LCE reached an inverted peak with a minimum value in the order of 10^2 kPa at the isotropic transition temperature, T_{ni}, above which all the mesogens become randomly

oriented. The isotropic transition is an indication of the presence of liquid crystalline order. The inverted peak was poorly defined for the RM80-PEG20 sample, as relatively high mesogen substitution led to the significant diminishing of the liquid crystalline order. Moreover, the negative peak was completely absent for the non-LCE sample RM0-PEG100 as all the rigid mesogens were substituted with the flexible backbone, and no liquid crystalline order was present. The inverted peak of E' and a small tan δ peak at T_{ni} are attributed to the instability of mesogen order at isotropic transition.[27,30,40,42] The instability of mesogens around T_{ni} arises from the possibility of mesogen rotation to either form ordered domains or become random.

Between the T_g and T_{ni}, the tan δ curve remained elevated at around 0.6 for an approximately 20°C temperature increment. This trend of the elevated tan δ curve can be attributed to the presence of an additional energy dissipation mechanism unique to LCE samples caused by mesogen rotation under mechanical loading. However, the absence of mesogens in the non-LCE RM0-PEG100 led to near-zero tan δ in the nematic-rubbery regime. At temperature above T_{ni}, all the mesogens became randomly oriented, and the LCE samples were in the isotropic phase. With further increase in temperature, the E' increased to above 10^3 kPa, which is dictated by the cross-link density of the LCE network.

The average transition temperatures for all the samples, based on the DMA tests, are listed in Table 1. With the increase in mesogen substitution, the average values of both T_g and T_{ni} decreased. The T_g slightly decreased from 4°C for RM100-PEG0 to −2°C for RM80-PEG20. However, the T_{ni} significantly decreased from 66°C to 23°C for no mesogen substitution to LCE with 20% mesogen substitution, respectively. The non-LCE RM0-PEG100 showed a relatively low T_g of −40°C, while the T_{ni} could not be measured due to an absence of any E' inverted peak.

The RM90-PEG10 sample showed an average T_{ni} of 32°C, slightly below the physiologically relevant temperature of 37°C, yet above a typical room temperature of 20°C. Therefore, this material can be potentially applied as a body temperature-induced reversible shifting material for biomedical applications. The RM90-PEG10 can be programmed to the desired shape and stored at room temperature, which will undergo nematic-isotropic transition and change shape at a temperature slightly below body temperature. This changed shape will be stable at body temperature as the material will be in the isotropic phase.

3.5 | Length actuation

The plots of length change as a function of temperature for representative samples are shown in Figure 5 (a), illustrating their shape-shifting capacity. The length change was not studied for non-LCE RM0-PEG100 as the shape could not be programmed. The curves for all samples showed 0% length change at temperatures above their corresponding T_{ni}, indicating no shape change occurs when the temperature is increased above isotropic. At this temperature, the samples assumed the shape of the polydomain sample obtained after the first-stage Michael Addition reaction. As the length change was measured along the stretching axis of the samples, the length of the sample was shortest above T_{ni}. When the samples were cooled, their length increased until reaching T_g, as the mesogens in the LCE were taking more ordered configuration with alignment along the stretching axis of the sample.[3,27,36] At temperatures below T_g, comparatively little change in length occurred with further

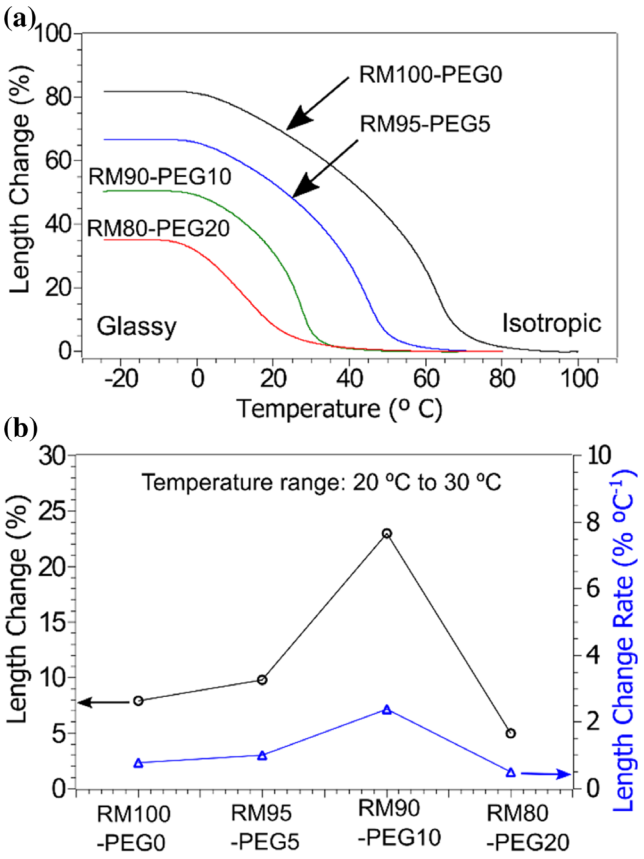

FIGURE 5 (a) Representative plots of length change as a function of temperature obtained for LCEs with varied rigid mesogen to flexible backbone ratio. An increase in mesogen substitution by flexible backbone led to a decrease in maximum length change in monodomain LCE, (b) average length change and rate of length change in 20°C–30°C temperature range are shown. RM90-PEG10 (i.e., monodomain LCE with a 10% mesogen substitution) sample showed the largest linear actuation within several seconds in this temperature range. LCE, liquid crystal elastomers [Color figure can be viewed at wileyonlinelibrary.com]

cooling. The length change values at this low-temperature plateau were the total shape change for the corresponding materials tested. With an increase in mesogen substitution, the average total shape changes decreased from 80% for RM100-PEG0 to 34% for RM80-PEG20. The candidate material for reversible shape change at body temperature, RM90-PEG10, showed a total of 50% length actuation, on average.

For all samples, the shape changes effectively occurred between the T_g and T_{ni} as length did not change above T_{ni} and below T_g. While the T_g remained relatively unchanged with mesogen substitution, the T_{ni} decreased significantly and hence dictated the shape-change temperature range. However, in practice, the temperature range for shape-shifting depends on the desired application. In this study, 20°C to 30°C was considered an appropriate temperature range for biomedical shape-shifting applications. This temperature range was chosen such that the shape-programmed sample will be stored at room temperature of 20°C, shape-shifting will be completed around 30°C, and the final shape will be stable at body temperature of 37°C.

The average length change and rate of length change in between 20°C and 30°C for all the different LCE samples are shown in Figure 5(b). In this temperature range, the RM90-PEG10 showed the length actuation of 23% within several seconds, at the rate of 2.3% $°C^{-1}$, most actuation among all materials tested.

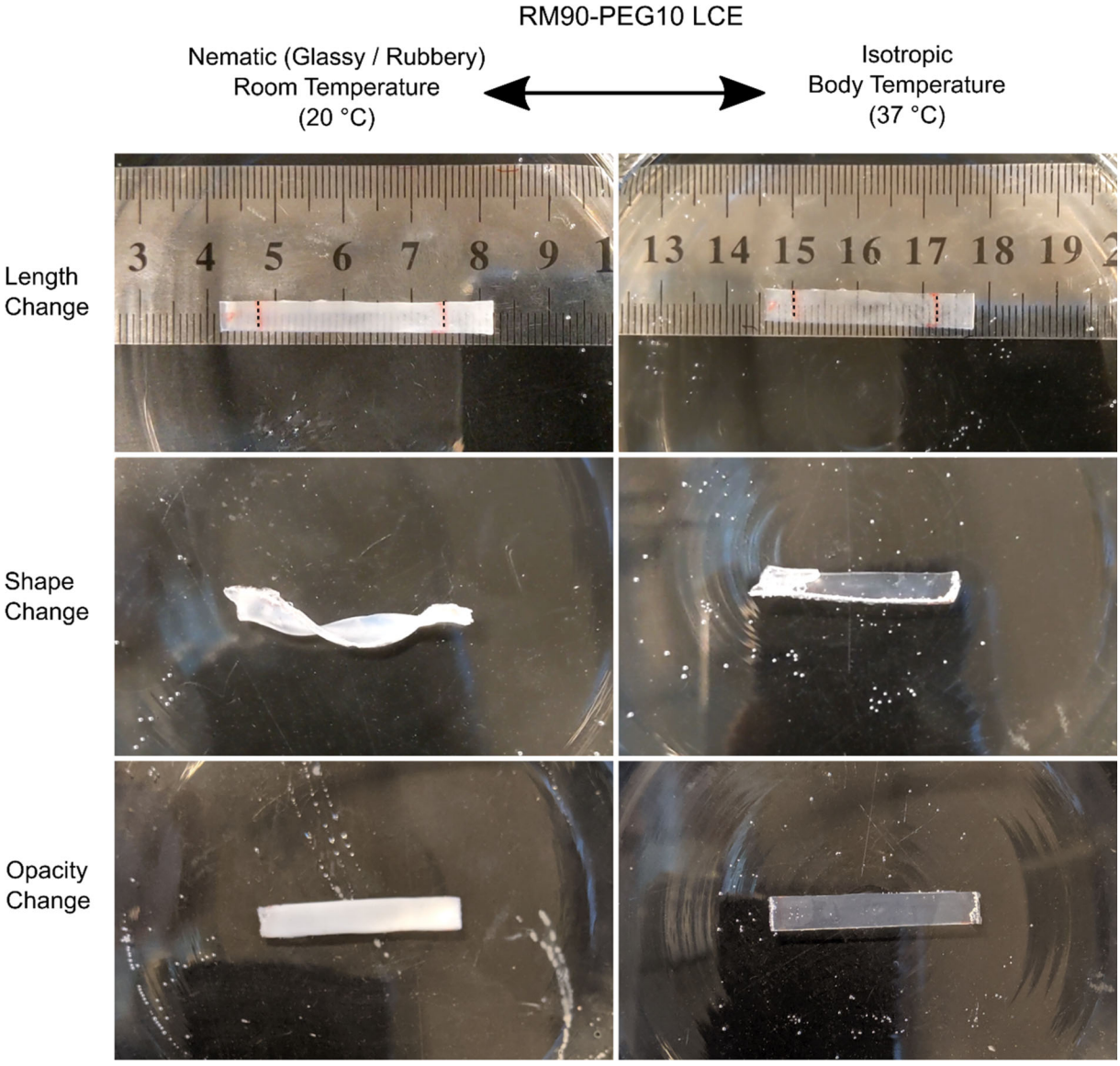

FIGURE 6 Reversible linear actuation, shape change, and opacity change of monodomain RM90-PEG10 (i.e., LCE with a 10% mesogen substitution) sample between nematic phase, that is, room temperature (20°C) and isotropic phase, that is, body temperature (37°C). LCE, liquid crystal elastomers [Color figure can be viewed at wileyonlinelibrary.com]

3.6 | Shape and opacity shifting

The length, shape, and opacity shifting of representative RM90-PEG10 samples in the temperature range between 20°C and 37°C are shown in Figure 6. The length change was demonstrated as the sample contracted when exposed at 37°C and expanded when cooled back at 20°C. Similarly, the shape change was observed as the twisted polydomain sample became straight at 37°C and recovered the twisted shape when exposed to 20°C. The opacity change was also observed as the fixed polydomain sample became transparent at 37°C and turned opaque white as placed back into a 20°C bath. All these transitions were observed to be reversible over at least 10 cycles.

The length, shape, and opacity change can be seen at real-time speed in Video S1, Video S2, and Video S3, respectively. All these changes were quick and reversible. These demonstrations indicated that RM90-PEG10 could potentially be applied where the material is required to respond to body temperature.

4 | DISCUSSION

The method described by Yakacki et al. utilizes a solvent that allows the Michael addition reaction in the first-stage to occur in a state where mesogens remain isotropic.[3] Later, Traugutt et al. adapted this method without using a solvent; however, the mesogens remain in a nematic state when the Michael addition reaction occurs.[40] In this study, we use the non-solvent based technique; however, we conduct the Michael addition reaction at a higher temperature such that the mesogens remain randomly oriented when the initial LCE network forms. Forming the initial LCE network with mesogens in the isotropic state typically shows advantageous behaviors such as more prominent nematic-isotropic transition and larger actuation compared to the nematic genesis.[20,40] Additionally, the non-solvent based method allows fabrication without necessitating subsequent extraction of solvents from the internal region of the sample, hence larger specimens can be produced easily. The absence of solvent also eliminates the possible release of unwanted solvents during potential biomedical applications. In a similar context, the high network conversion results from the Michael addition reaction limits the release of potentially harmful unreacted chemicals when applied as biomaterials.

To study the effect of the substitution of rigid mesogen with a flexible backbone, RM257 was systematically substituted with PEGDA250. The PEGDA250 was chosen as it is a widely used chemical for biomedical studies, which has the same number of acrylate functional groups as the RM257. The PEGDA250 is a flexible monomer due to the absence of any rigid aromatic or aliphatic rings in the structure. Additionally, the PEGDA250 is much less hydrophilic compared to the higher molecular weight equivalents and effectively insoluble to water.[46] Therefore, PEGDA250 should discourage body fluid absorption during potential biomedical applications of the LCE.

To consider the LCEs explored in this work for biomedical applications, its potential biocompatibility is a crucial factor. LCE with very similar constituents and fabrication method has been proven to be non-cytotoxic via in vitro studies[3] and biocompatible via *in vivo* study.[19] The previously studied LCE also showed minimal swelling when exposed to the physiological condition.[19] The LCE discussed in the current study also expected to be biocompatible, as only new constituent PEGDA is reported to be cytocompatible.[41,47]

The partial substitution of the rigid mesogens with the flexible backbone, at least up to 80% substitution studied in this work, did not completely diminish the liquid crystalline order, as can be seen from the POM images (Figure 3). The brightness of the POM images was unable to reliably reveal the degree of the mesogen order as the thicknesses of the samples were not strictly the same. When a quantitative measure of the mesogen order is desired, wide-angle X-ray scattering (WAXS) has been used in the literature.[3,27,36,44] However, this study focused on DMA to directly study the effect on the transition temperatures.

It can be assumed that the mesogen substitution and increase of the flexible components led to lower mesogen concentration, therefore, more spacing between the mesogens. With decreasing mesogen concentration and the increasing mesogen spacing, the mesogens in the localized domains are expected to become less ordered. Consequently, the polydomain samples after the first-stage showed narrower soft elasticity for increased mesogen substitution (Figure 2(a)). This effect of the increase in rigid mesogen substitution on the narrowing of the soft elasticity is similar to the effect of the increasing cross-link density[30] and the rise in testing temperature.[48] The introduction of lower molecular weight and flexible PEG250 into the polymer backbone may have led to a tighter network and limited mesogen motion, similar to increasing cross-link density. Also, many researchers discussed that the mesogen order in domains is disrupted with the increase in temperature.[29,37,42,49] The disrupted mesogen order forces the polydomain LCEs to show narrower soft elasticity when tested at increasing temperature, below the T_{ni}.[48] In this work, the soft elasticity of all the materials was tested at room temperature, while

the T_{ni} decreased for samples with increased mesogen substitution. Therefore, the test temperature was effectively closer to the corresponding T_{ni} for samples with increased mesogen substitution, which have inherently contributed to the narrowing of the soft elastic plateau. Furthermore, the polydomain LCEs show no soft elasticity and become relatively brittle at a temperature above $T_{ni,}$[48] similar to the RM0-PEG100 sample studied here. This lack of soft elasticity and brittleness of LCEs above the T_{ni} and for RM0-PEG100 samples can be attributed to the lack of liquid crystalline order in the isotropic phase or the absence of liquid crystallinity promoting mesogens altogether.

The decrease in the T_{ni} with increasing mesogen substitution observed in this study (Figure 4), can also be explained with the possible rise of less ordered domains. It should be easier to completely diminish the mesogen order when the mesogens are already less ordered, hence can be achieved at a lower temperature. However, the substitution of mesogen with a flexible backbone affected the T_{ni} more significantly than the T_g. The mobility of the network chains dictates the T_g of a polymer network. Upon partial substitution of the mesogen, up to 20% in this study, the majority portion of the LCE network still consists of the bulky and rigid mesogens. Therefore, the network mobility can be expected to increase slightly, and the T_g to decreases. However, adding the smaller and flexible PEG250 monomers decrease the average molecular weight between the cross-links and can increase inherent cross-link density, leading to a slightly T_g increasing effect. Combining the competing effects, the T_g was observed to decrease only marginally. On the contrary, a relatively small amount of mesogen substitution acts to disrupt the mesogen order; consequently, T_{ni} was lowered significantly. However, when all the mesogens were substituted with a flexible backbone, the network mobility changed significantly. The molecular weight of PEG is 250 g/mol, almost half when compared to the molecular weight of 589 g/mol for RM257. The much lower molecular weight of the flexible PEG chains may have led to a decrease of T_g from 4°C to −40°C, for RM100-PEG0 and RM0-PEG100, respectively.

In this study, the overall shape-programming capacity (i.e., fixed strain), shape-retention capacity (i.e., fixity), and shape-shifting capacity (i.e., total length change) of the LCEs were observed to decrease as the rigid mesogens were substituted with a flexible backbone. The fixity did not decrease as drastically as the fixed strain because the applied strain decreased with increased mesogens substitution as well. The shape actuation of the LCEs depends on the degree of mesogen order in the domains of polydomain LCEs after the first-stage. Therefore, the lower fixed strain and decreased total length change can be considered as a direct implication of diminished mesogen concentration and narrower soft elasticity occurring from lower mesogen content.

For a specific LCE, the maximum shape-shifting can be captured if the full range of shape-changing temperature, that is, T_g to $T_{ni,}$ can be utilized during application. Furthermore, the shape-shifting occurs quickly with respect to temperature near the $T_{ni.}$[27] Therefore, the LCEs with T_{ni} above the body temperature may show a partial change in shape upon implantation in the body; however, the changed shape will be unstable, and the rate of shape change will be very slow. Additionally, in this case, the opacity change will be very limited. To efficiently capture the shape-shifting of LCEs for biomedical applications, the nematic phase should be stable at storage and programming temperature. At the same time, the nematic-isotropic transition should happen at a temperature slightly below body temperature. The T_{ni} being slightly below body temperature will allow complete and maximum shape-shifting, as well as a stable shape during application.

RM90-PEG10, the candidate body-temperature shape-shifting LCE in this study, was shape programmed and stored at room temperature (20°C), where it is in the nematic phase. The T_{ni} for RM90-PEG10 was 32°C, which was slightly below the human body temperature (37°C). The RM90-PEG10 shows a gradual and total of 50% length actuation in the full temperature range between the T_g of 3°C and T_{ni} of 32°C. However, almost half of the length change (23% length change) happens between 20°C and 30°C. Therefore, the full range of shape-shifting is not utilized as the sample is stored at 20°C, instead of the T_g of 3°C. The shape-shifting steps during the potential applications can be described as follows – (1) at first, the material with a programmed shape (shape after second-stage) is stored at 20°C. It is noted that the material has changed the shape by an unutilized amount between the T_g and storage temperature, as the storage temperature is higher than T_g. (2) Next, the material is introduced at body temperature, the temperature of the material will increase, and the material will change shape by about 23% between the 20°C and 30°C. (3) With the further increase in temperature, the material will eventually reach the isotropic phase at around 32°C, and shape change will finish. At temperatures above 32°C, that is, around body temperature of 37°C, the material will completely be in the isotropic phase, and the changed shape will stabilize.

The RM90-PEG10 demonstrated quick and complete length, shape, and opacity changes between 20°C and 37°C (Figure 6, Video S1, Video S2, and Video S3). These transitions can potentially be utilized in biomedical applications, including stent-graft, blood clot removal device,

self-tightening suture, etc. For a stent-graft application, a tube-shaped LCE (after first-stage) can be folded to a small size for ease of insertion, and the folded shape can be programmed (second-stage). The folded shape of the stent-graft will be stable at room temperature. Once inserted into the body, the stent-graft will extend and retain the before-programmed tube shape (after first-stage). For a blood clot removal device, a spiral-shaped LCE can be made (after first-stage), followed by programming to a straight-shape (after second-stage). The straight-shape, stable at room temperature, will allow ease of insertion, and the LCE will go back to the spiral shape when inserted into the body. For a self-tightening suture, monofilament LCE (after first-stage) can be programmed to an elongated shape (after second-stage). Once the wound is closed with elongated LCE suture, the suture will contract and tighten the stitches.

However, to develop a biomedical application using the LCEs described in this study, long-term biocompatibility and effect of exposure to the physiological condition should be investigated in future studies. Additionally, a similar study with different sized mesogens and different network compositions should be conducted to explore other possible body-temperature and various application-specific shape-shifting LCEs.

5 | CONCLUSION

In this study, an LCE with reversible shape-shifting around human body temperature was developed by tuning the nematic-isotropic transition temperature (T_{ni}) to slightly below the body temperature, yet above the room temperature. To tailor the T_{ni}, the rigid mesogens of the LCEs were systematically substituted with flexible backbones. The increasing mesogen substitution decreased the span of the soft elastic plateau, fixed strain, and fixity. The POM imaging revealed the presence of liquid crystalline order in LCEs with partially substituted mesogens. Additionally, the T_{ni} decreased from 66°C to 23°C by 20% substitution of rigid mesogen RM257 with flexible backbone PEGDA250. A material with a 10% mesogen substituted showed T_{ni} of 32°C. This material was identified for body temperature shape-shifting applications, and the linear actuation, shape-shifting, and opacity shifting were investigated between room temperature and body temperature. With the aim of biomedical applications, future work will involve studying long-term biocompatibility and the effect of exposure to physiological conditions. Other possible body-temperature shape-shifting LCEs will also be explored in future studies by using different sized mesogens and different network compositions.

ACKNOWLEDGMENT

The authors appreciate the funding support from the NSF-PFI grant (Grant No. 1827288). The authors thank Margaret R. Lichtenfels for her help with the experiments.

CONFLICT OF INTEREST

The authors have no conflicts to declare.

ORCID

Rajib K. Shaha https://orcid.org/0000-0001-6136-8958
Carl P. Frick https://orcid.org/0000-0002-8202-924X

REFERENCES

[1] T. Chung, A. Romo-Uribe, P. T. Mather, *Macromolecules* **2008**, *41*, 184.
[2] A. Kirillova, L. Ionov, *J. Mater. Chem. B* **2019**, *7*, 1597.
[3] C. M. Yakacki, M. Saed, D. P. Nair, T. Gong, S. M. Reed, C. N. Bowman, *RSC Adv.* **2015**, *5*, 18997.
[4] H. Jiang, C. Li, X. Huang, *Nanoscale* **2013**, *5*, 5225.
[5] M. Barnes, S. Sajadi, S. Parekh, M. M. Rahman, P. M. Ajayan, R. Verduzco, *ACS Appl. Mater. Interfaces* **2020**, *12*, 28692.
[6] M. O. Saed, E. M. Terentjev, *ACS Macro Lett.* **2020**, *9*, 749.
[7] F. Ge, Y. Zhao, *Adv. Funct. Mater.* **2019**, *30*, 1901890.
[8] Y. Shang, J. Wang, T. Ikeda, L. Jiang, J. M. Chem, Y. Shang, J. Wang, T. Ikeda, L. Jiang, *J. Mater. Chem. C* **2019**, *7*, 3413.
[9] M. T. Brannum, A. M. Steele, M. C. Venetos, L. S. T. J. Korley, G. E. Wnek, T. White, *J. Adv. Opt. Mater.* **2019**, *7*, 1801683.
[10] S. M. Clarke, A. R. Tajbakhsh, E. M. Terentjev, C. Remillat, G. R. Tomlinson, J. R. House, *J. Appl. Phys.* **2001**, *89*, 6530.
[11] N. A. Traugutt, D. Mistry, C. Luo, K. Yu, Q. Ge, C. M. Yakacki, *Adv. Mater.* **2020**, *32*, 2000797.
[12] P.-G. De Gennes, M. Hébert, R. Kant, *Macromol. Symp.* **1997**, *113*, 39.
[13] H. Wermter, H. Finkelmann, *E-Polymers* **2001**, *1*, 1.
[14] M.-H. Li, P. Keller, *Philos. Trans. R. Soc. A Math. Phys. Eng. Sci.* **2006**, *364*, 2763.
[15] M. E. Prévôt, S. Ustunel, E. Hegmann, *Materials (Basel).* **2018**, *11*, 377.
[16] Y. Inoue, Y. Atsumi, A. Kawamura, T. Miyata, *J. Memb. Sci.* **2019**, *588*, 117213.
[17] C. Ferrantini, J. M. Pioner, D. Martella, R. Coppini, N. Piroddi, P. Paoli, M. Calamai, F. S. Pavone, D. S. Wiersma, C. Tesi, E. Cerbai, C. Poggesi, L. Sacconi, C. Parmeggiani, *Circ. Res.* **2019**, *124*, e44.
[18] R. H. Volpe, D. Mistry, V. V. Patel, R. R. Patel, C. M. Yakacki, *Adv. Healthc. Mater.* **2020**, *9*, 1901136.
[19] R. K. Shaha, D. R. Merkel, M. P. Anderson, E. J. Devereaux, R. R. Patel, A. H. Torbati, N. Willett, C. M. Yakacki, C. P. Frick, *J. Mech. Behav. Biomed. Mater.* **2020**, *107*, 103757.
[20] K. Urayama, E. Kohmon, M. Kojima, T. Takigawa, *Macromolecules* **2009**, *42*, 4084.
[21] F. Elias, S. M. Clarke, R. Peck, E. M. Terentjev, *Europhys. Lett.* **1999**, *47*, 442.
[22] S. M. Clarke, E. M. Terentjev, I. Kundler, H. Finkelmann, *Macromolecules* **1998**, *31*, 4862.
[23] A. Buguin, M. H. Li, P. Silberzan, B. Ladoux, P. Keller, *J. Am. Chem. Soc.* **2006**, *128*, 1088.

[24] J. M. Boothby, H. Kim, T. H. Ware, *Sensors Actuators, B Chem.* **2017**, *240*, 511.
[25] R. S. Kularatne, H. Kim, J. M. Boothby, T. H. Ware, *J. Polym. Sci. Part B Polym. Phys.* **2017**, *55*, 395.
[26] C. Ohm, M. Brehmer, R. Zentel, *Adv. Mater.* **2010**, *22*, 3366.
[27] D. R. Merkel, N. A. Traugutt, R. Visvanathan, C. M. Yakacki, C. P. Frick, *Soft Matter* **2018**, *14*, 6024.
[28] M. O. Saed, C. P. Ambulo, H. Kim, R. De, V. Raval, K. Searles, D. A. Siddiqui, J. M. O. Cue, M. C. Stefan, M. R. Shankar, T. H. Ware, *Adv. Funct. Mater.* **2019**, *29*, 1806412.
[29] M. Warner, E. M. Terentjev, *Oxford university press* **2007**, *120*, 136.
[30] M. O. Saed, A. H. Torbati, C. A. Starr, R. Visvanathan, N. A. Clark, C. M. Yakacki, *J. Polym. Sci. Part B Polym. Phys.* **2017**, *55*, 157.
[31] M. Bispo, D. Guillon, B. Donnio, H. Finkelmann, *Macromolecules* **2008**, *41*, 3098.
[32] T. H. Ware, M. E. McConney, J. J. Wie, V. P. Tondiglia, T. J. White, *Science* **2015**, *347*, 982.
[33] A. Sánchez-Ferrer, H. Finkelmann, *Mol. Cryst. Liq. Cryst.* **2009**, *508*, 710.
[34] I. A. Rousseau, P. T. Mather, *J. Am. Chem. Soc.* **2003**, *125*, 15300.
[35] A. Lebar, Z. Kutnjak, S. Žumer, H. Finkelmann, A. Sánchez-Ferrer, B. Zalar, *Phys. Rev. Lett.* **2005**, *94*, 197801.
[36] M. O. Saed, R. H. Volpe, N. A. Traugutt, R. Visvanathan, N. A. Clark, C. M. Yakacki, *Soft Matter* **2017**, *13*, 7537.
[37] S. Krause, F. Zander, G. Bergmann, H. Brandt, H. Wertmer, H. Finkelmann, *Comptes Rendus Chim.* **2009**, *12*, 85.
[38] D. Lacey, H. N. Beattie, G. R. Mitchell, J. A. Pople, *J. Mater. Chem.* **1998**, *8*, 53.
[39] B. Rožič, S. Krause, H. Finkelmann, G. Cordoyiannis, Z. Kutnjak, *Appl. Phys. Lett.* **2010**, *96*, 2.
[40] N. A. Traugutt, R. H. Volpe, M. S. Bollinger, M. O. Saed, A. H. Torbati, K. Yu, N. Dadivanyan, C. M. Yakacki, *Soft Matter* **2017**, *13*, 7013.
[41] J. L. Drury, D. J. Mooney, *Biomaterials* **2003**, *24*, 4337.
[42] A. Lebar, G. Cordoyiannis, Z. Kutnjak, B. Zalar, in *Liquid Crystal Elastomers: Materials and Applications* (Ed: W. H. Jeu), Springer, Berlin, Heidelberg **2012**, p. 147.
[43] P. Palffy-Muhoray, in *Liquid Crystal Elastomers: Materials and Applications* (Ed. W. H. Jeu), Springer, Berlin, Heidelberg, **2012**, p. 95.
[44] A. H. Torbati, P. T. Mather, *J. Polym. Sci. Part B Polym. Phys.* **2016**, *54*, 38.
[45] T. H. Ware, Z. P. Perry, C. M. Middleton, S. T. Iacono, T. White, *J. ACS Macro Lett.* **2015**, *4*, 942.
[46] C. Nam, J. Yoon, S. A. Ryu, C.-H. Choi, H. Lee, *ACS Appl. Mater. Interfaces* **2018**, *10*, 40366.
[47] R. K. Shaha, Z. Jiang, C. P. Frick, J. Oakey, *ACS Appl. Polym. Mater.* **2019**, *1*, 2571.
[48] D. R. Merkel, R. K. Shaha, C. M. Yakacki, C. P. Frick, *Polymer (Guildf).* **2019**, *166*, 148.
[49] V. S. R. Jampani, R. H. Volpe, K. Reguengo de Sousa, J. Ferreira Machado, C. M. Yakacki, J. P. F. Lagerwall, *Sci. Adv.* **2019**, *5*, eaaw2476.

SUPPORTING INFORMATION

Additional supporting information may be found online in the Supporting Information section at the end of this article.

How to cite this article: Shaha RK, Torbati AH, Frick CP. Body-temperature shape-shifting liquid crystal elastomers. *J Appl Polym Sci*. 2021;138: e50136. https://doi.org/10.1002/app.50136